Chemistry & Biology
Article

Sterol 14α-Demethylase as a Potential Target for Antitrypanosomal Therapy: Enzyme Inhibition and Parasite Cell Growth

Galina I. Lepesheva,[1,*] Robert D. Ott,[2] Tatiana Y. Hargrove,[1] Yuliya Y. Kleshchenko,[3] Inge Schuster,[4] W. David Nes,[5] George C. Hill,[2] Fernando Villalta,[3] and Michael R. Waterman[1]
[1]Department of Biochemistry
[2]Department of Microbiology and Immunology
Vanderbilt University School of Medicine, Nashville, TN 37232-0146, USA
[3]Department of Microbial Pathogenesis and Immune Response, Meharry Medical College, Nashville, TN 37208, USA
[4]Institute of Pharmaceutical Chemistry, University Vienna, Oesterreich, Austria
[5]Department of Chemistry and Biochemistry, Texas Tech University, Lubbock, TX 79409, USA
*Correspondence: galina.i.lepesheva@vanderbilt.edu
DOI 10.1016/j.chembiol.2007.10.011

SUMMARY

Sterol 14α-demethylases (CYP51) serve as primary targets for antifungal drugs, and specific inhibition of CYP51s in protozoan parasites *Trypanosoma brucei* (TB) and *Trypanosoma cruzi* (TC) might provide an effective treatment strategy for human trypanosomiases. Primary inhibitor selection is based initially on the cytochrome P450 spectral response to ligand binding. Ligands that demonstrate strongest binding parameters were examined as inhibitors of reconstituted TB and TC CYP51 activity in vitro. Direct correlation between potency of the compounds as CYP51 inhibitors and their antiparasitic effect in TB and TC cells implies essential requirements for endogenous sterol production in both trypanosomes and suggests a lead structure with a defined region most promising for further modifications. The approach developed here can be used for further large-scale search for new CYP51 inhibitors.

INTRODUCTION

Trypanosomatidae cause endemic infections and countless human deaths over the world (http://www.emedicine.com/). Sleeping sickness, or African trypanosomiasis (causative agent *Trypanosoma brucei* [TB]), and Chagas disease, or American trypanosomiasis (*Trypanosoma cruzi* [TC]), are most abundant. The parasites have complex lifecycles using insects, tsetse fly (TB) and triatomine bugs (TC), as vectors, humans, and a variety of mammals as hosts. In humans, TB remains extracellular, the chronic stage of the disease beginning when the pathogen crosses the blood/brain barrier and invades the central nervous system. TC affects the heart and gastrointestinal tract and at the chronic stage is found mainly as an intracellular amastigote. Currently ~60 million people in Sub-Saharan Africa are at risk of sleeping sickness, 0.3–0.5 million new cases occurring each year. Sixteen to eighteen million people in Central and South America are infected with TC with an annual incidence of 0.2 million new cases. In the US, Chagas disease predominantly exists as a result of immigration, blood transfusion, or organ transplantation; however, autochthonous cases of the infection have also been reported in several states [1–4]. There are no vaccines for these diseases and only a very limited set of drugs; four for sleeping sickness (suramin [since 1916], pentamidine [1941], melarsoprol [1949], eflornithine [1990]) and two for Chagas disease (nifurtimox [since 1972] and benznidazole [1978]) (Figure S1, see the Supplemental Data available with this article online). These drugs are inadequate because of high toxicity, side effects, difficulties with administration, resistance, and low or no efficacy at the prevalent chronic stages, which are commonly fatal. New, more efficient medications for antitrypanosomal therapy are urgently needed [1, 5–8].

One of the approaches for rational design of antitrypanosomal drugs is to specifically block an essential enzyme or metabolic pathway in the parasite. Being required in most eukaryotic kingdoms, sterol biosynthesis is one such possible target. The pathway leads to production of cholesterol in mammals, ergosterol in fungi, and a variety of 24-alkylated and olephynated sterols in plants and protists [9, 10]. Cholesterol, ergosterol, and sitosterol (plants) are essential structural components of plasma membranes. These structural sterols stabilize membranes, determine their fluidity and permeability, and modulate activity of membrane-bound enzymes and ion channels. In addition, sterols serve as precursors for bioactive molecules, which function at nanomolar hormonal levels as regulators of cell cycle and development [10, 11]. While mammals can accumulate cholesterol from the diet, blocking of ergosterol production in fungi is lethal; it affects cytokinesis, stops cell growth, and eventually leads to a collapse of the cellular membrane [9, 11]. Inhibitors of sterol biosynthesis are currently the most widely used clinical and agricultural antifungal agents [12].

Positive results of use of inhibitors of fungal sterol biosynthetic enzymes for potential treatment of protozoan infections have been obtained for TC [13–22] and Leishmania species [23–25]. As for TB, it has been reported that contrary to procyclic (insect) forms, bloodstream (mammalian) stages of the parasite lifecycle do not synthesize endogenous sterols but use host cholesterol to build their membranes [26, 27]. However, recent experiments have demonstrated that inhibitors of fungal sterol 24-methyltransferase are effective in killing bloodstream forms of TB [28, 29].

Sequencing of TB and TC genomes [7] revealed presence of all sterol biosynthetic enzymes in the parasites including sterol 14α-demethylase (CYP51), a cytochrome P450 that functions at the initial stages of the specific postsqualene portion of the pathway, catalyzing a three-step reaction of oxidative removal of the 14α-methyl group from the newly cyclized sterol precursors [30]. CYP51 is a primary target for azole derivatives in antifungal therapy. Inhibition of the CYP51 reaction in fungi leads to accumulation of 14α-methylated sterols, which are unable to replace ergosterol in the membrane because of steric hindrance [11].

CYP51s from TB and TC have only ~25% amino acid identity to their fungal orthologs and are 83% identical to each other. We have shown that while TCCYP51 expresses preference towards the C4-dimethylated 24-methylenedihydrolanosterol, the natural substrate of CYP51 from filamentous fungi, TBCYP51 is strictly specific toward the C4-monomethylated plant-like substrates (obtusifoliol and norlanosterol) and that based on amino acid sequence all other sequenced protozoan CYP51 will resemble the TBCYP51 in activity [31–33].

In this study, correlation between specific inhibition of trypanosomal CYP51 and antiparasitic effect on trypanosomal cells has been investigated. Using antifungal drugs ketoconazole and fluconazole as controls, a selection of fifteen novel imidazole derivatives from Novartis, found to cause strong spectral responses in highly purified TB and TC CYP51 ($K_{d[P450\text{-}azole]} < K_{d[P450\text{-}substrate]}$), were further examined as inhibitors of reconstituted TB and TC CYP51 activity in vitro. In accordance with binding parameters, the compounds produced a profound effect on the initial rates of catalysis of both trypanosomal CYP51s. In most cases, no excess of the inhibitor over the enzyme was required to cause a 2-fold decrease in the rate of substrate conversion. Time-course experiments, however, revealed significant divergence in their potencies, often contradicting the K_d values and suggesting that determination of an inhibitory potency as the influence on maximal CYP51 turnover can be misleading. More detailed analysis of azole structure/inhibitory effect relationship has shown that while the presence of a bulky aromatic structure in either α or β position relative to the imidazole ring is required for efficient binding, the azoles having an α-phenyl group can be easily replaced by substrate in the reconstituted enzyme reaction. However, switching the phenyl group to the β-position converts them into much more potent CYP51 inhibitors, sometimes having virtually irreversible action. Ketoconazole and selected experimental compounds were further tested in TB and TC cells and found to be effective growth inhibitors, cellular drug sensitivities correlating with the long-term inhibitory effect observed on CYP51 activity in vitro.

RESULTS AND DISCUSSION

CYP51 Spectral Response to Ligand Binding as a Basis for the Initial Screening

By mechanism of action, azoles belong to the group of reversible competitive inhibitors of cytochromes P450 [34]. The unsubstituted basic nitrogen forms the sixth (axial) coordination bond with the heme iron blocking binding and activation of molecular oxygen and preventing accommodation of the substrate in the active center. The inhibitory effect strongly depends on the size and configuration of the N-substituted part of the azole molecule, which forms multiple additional interactions with the protein moiety of the cytochrome P450. Thus, the inhibitory effect of small molecules such as imidazole or phenylimidazoles is very weak, while much bulkier ketoconazole serves as a potent antifungal drug but has rather low selectivity; in addition to CYP51, it was also found to strongly inhibit other human P450s [35].

Being highly hydrophobic, membrane-bound enzymes metabolizing substrates of extremely low solubility in aqueous solutions, fungal CYP51s are quite resistant to purification (so far, purification of only three fungal CYP51 orthologs was reported [30]) and also often to reconstitution of activity in vitro. Because of these problems, inhibitory potencies of azole drugs are mainly compared indirectly as their effects on fungal strain growth (e.g., [11, 36–39]). Though not normalized per equal amount of P450, the data imply that potencies of the same azole on CYP51s from different fungal species can vary significantly, differences up to three orders of magnitude have been reported [11, 34]. The latter means that highly selective strong CYP51 inhibition can be potentially reached as a result of maximal correspondence between the structure of an azole derivative and the topology of the target P450 substrate binding cavity. The needs for selective CYP51 inhibitors are growing sharply because such compounds would increase the efficiency and shorten the time necessary for treatment, which in turn can prevent the development of drug resistance, which is one of the most severe problems in clinical antifungal therapy (especially in treatment of immunocompromised patients) and in agriculture [40].

As a cysteine-coordinated hemoprotein, sterol 14α-demethylase responds spectrally to any perturbations in the area surrounding the heme iron (Figure 1). These spectral responses, type 1 for the interaction with the substrate and type 2 for interaction with an azole inhibitor, can be used to estimate the apparent dissociation constants (K_d) of the enzyme/ligand complexes. Thirty imidazole derivatives from a Novartis program on inhibitors of vitamin D hydroxylases [41, 42] were tested for spectral responses in highly purified TB and TC CYP51. Eleven compounds

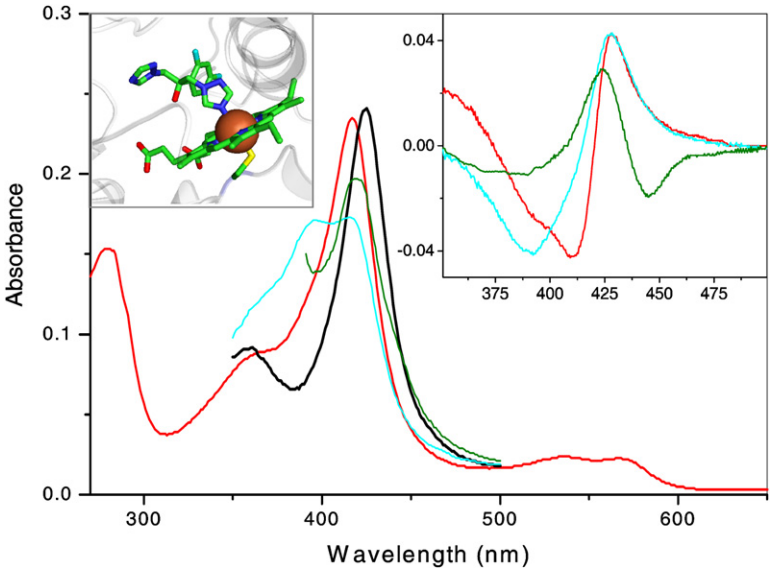

Figure 1. CYP51 Absorbance upon Alterations in the Heme and Its Environment

Main panel, absolute spectra of 2 μM TBCYP51: oxidized ligand free (red), reduced ligand free (green), oxidized 47% high-spin obtusifoliol bound (cyan), azole **4** bound (black). Blue shift in the Soret band maximum (from 417 to 394 nm) is caused by expulsion of a water molecule from the sixth coordination sphere of the heme iron (e.g., by substrate, which itself does not form a coordination bond with the iron). This spectral response (type 1) reflects transition of the iron from the hexa-coordinated low-spin state to the penta-coordinated high-spin state. Direct coordination of a basic atom (e.g., aliphatic or aromatic nitrogen) to the heme iron causes a red shift in the Soret band (to 426–429 nm) also known as type 2 response in the difference spectra. Right inset, type 2 difference spectra observed upon azole binding to oxidized, reduced, and substrate-bound TBCYP51 (color code as above). Left inset, coordination of fluconazole to the heme iron in the crystal structure of the CYP51 from *Mycobacterium tuberculosis* [1ea1]. The iron is shown as brown sphere, the heme-coordinated Cys residue (fifth axial ligand) is located beneath the iron, the sulfur atom is colored in yellow, protein moiety is shown in grey.

(Figure 2A) demonstrated high binding affinities (the K_ds being close or lower than the K_ds calculated from type 1 spectral responses of TB and TC CYP51 to their substrates) and were chosen for further testing as potential inhibitors. Antifungal drugs ketoconazole and fluconazole served as controls. Supporting the notion that the affinities of azole/CYP51 interactions can be species specific, the estimated apparent K_d of these compounds to the protozoan CYP51s are often more than one order of magnitude lower than the values obtained for the CYP51 from *Mycobacterium tuberculosis* (26% amino acid identity) and in many cases significantly lower than those calculated for the human ortholog (27% identity to TB/TC CYP51) (Table S1). Comparing the K_ds calculated for the two trypanosomal CYP51s, only compounds **1**, **11**, and especially ketoconazole show higher affinity toward the TC ortholog, the rest of the azoles produce rather similar K_ds in both enzymes, the best values (compounds **4** and **10**) being ~20-fold lower than the K_ds for the interaction of TB and TC CYP51 with their substrates.

Identification of the Most Potent CYP51 Inhibitors

Estimation of the Inhibitory Potency in the Reconstituted Enzyme Reaction In Vitro

In accordance with their high binding affinity, the compounds produced strong inhibitory effect on the initial rates of catalysis. The molar ratios inhibitor/enzyme required to slow down the reaction 2-fold (I/E_2) were lower than one in all cases except for compound **5** (for both trypanosomal CYP51s), ketoconazole, and fluconazole for the TB ortholog (Figure 2).

The reaction conditions used to reconstitute the CYP51 activity are optimized to give maximal turnover and reproducibility [30]. Low solubility of the sterols limits maximal substrate concentration to 50 μM, while decrease in the enzyme concentration affects stability and protein-protein interactions with the electron donor, cytochrome P450 reductase. Because of these restrictions, time-course experiments were undertaken to increase sensitivity of the assay in order to distinguish the most potent inhibitors. The results revealed significant divergence in the potencies of the compounds assayed. However, I/E_2 determined as the molar ratio inhibitor/enzyme required for reaching a 2-fold decrease in the substrate conversion per 1 hr often demonstrated lack of correspondence with the relative apparent K_d values (Figure 2, numbers in brackets). Though certain increase in the I/E_2 ratios estimated for long-term incubations was expected as a result of substrate depletion, no such changes were registered for compounds **2** and **4**. Stronger inhibitory effect than could be predicted from the K_d was demonstrated by **1**, especially on TBCYP51. On the contrary, compounds **6–10**, regardless of the variations in their K_ds, all show a similar rapid time-dependent increase in the I/E_2.

Clearly the best inhibitors are distinguished over time upon comparison of the effects of the azoles at equimolar ratio to the enzymes (Figure 3). Under this condition, no substrate conversion can be detected even after 1 hr reaction when compounds **2** or **4** are added. Incubation intervals up to 4 hr were tested with the same result, while more than 90% of the enzyme in the reaction remains in the active P450 form. Thus, within the time tested, the effect

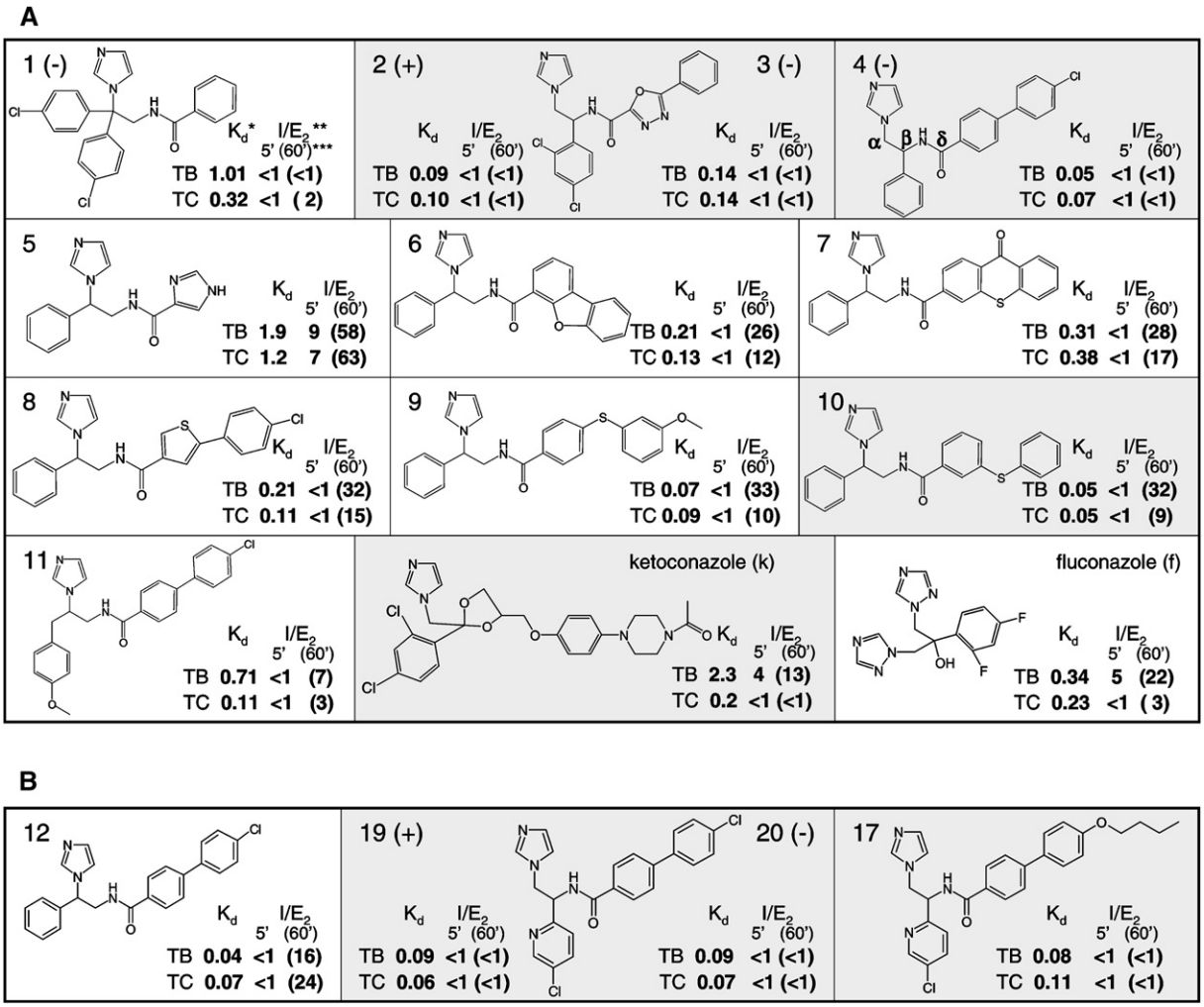

Figure 2. Azole Derivatives Assayed as Potential Inhibitors of TB and TCCYP51

(A) Compounds selected based on the binding affinities estimated from the P450 spectral responses. The compounds used in cellular studies are marked with grey background. Asterisk, apparent dissociation constants, μM. Inhibitory effects of azoles with Kds higher than the Kds for the enzyme/substrate complexes (1.2 and 0.8 μM for the interaction of TBCYP51 with obtusifoliol and TCCYP51 with 24-methylenedihydrolanosterol, respectively [31, 32]) were much weaker; compound **5** is included as an example. Double asterisk, molar ratio inhibitor/P450 which produces a 2-fold decrease in the activity. Triple asterisk, I/E_2 calculated as the influence on the initial rate (5′) of catalysis (I/E_2 calculated as the influence on the percentage of substrate conversion after 1 hr [60′] reaction). The results of four experiments are presented as mean; standard deviation does not exceed 10%.

(B) Azoles added after structure/activity relation analysis.

of compounds **2** and **4** on both trypanosomal CYP51s remains irreversible.

The Affinity of the Azole-CYP51 Interaction Can Change under the Reaction Conditions

To understand the reasons for the observed discrepancies between the apparent K_ds and inhibitory effects on the CYP51 activity, we tested stability of compounds **4** (long-term inhibitor) and **10** (short-term inhibitor) in the reaction mixture and compared influence of substrate and P450 reduction on the relative affinities of their interaction with TBCYP51 (spectral responses of substrate-bound and $Na_2S_2O_4$-reduced TBCYP51 to the azole binding are shown in Figure 1, insert). No trace of metabolism or decomposition during the reaction time was detected for either azole. Excess of substrate, however, was found to result in a 13-fold higher increase in the calculated K_d upon titration of TBCYP51 with **10** than upon titration with **4** (Table 1). If the substrate was added after the azole, it did not cause spectral changes when TBCYP51 was bound with **4** but produced time-dependent type 1 response in the case of **10**. A negative effect of P450 reduction on the interaction with **10** was also stronger, 4-fold increase in the apparent K_d versus only 1.5-fold increase in the case of compound **4**. Again, if TBCYP51 was reduced after the titration with the azoles and then exposed to CO, the rate and efficiency of the CO-complex formation [43]

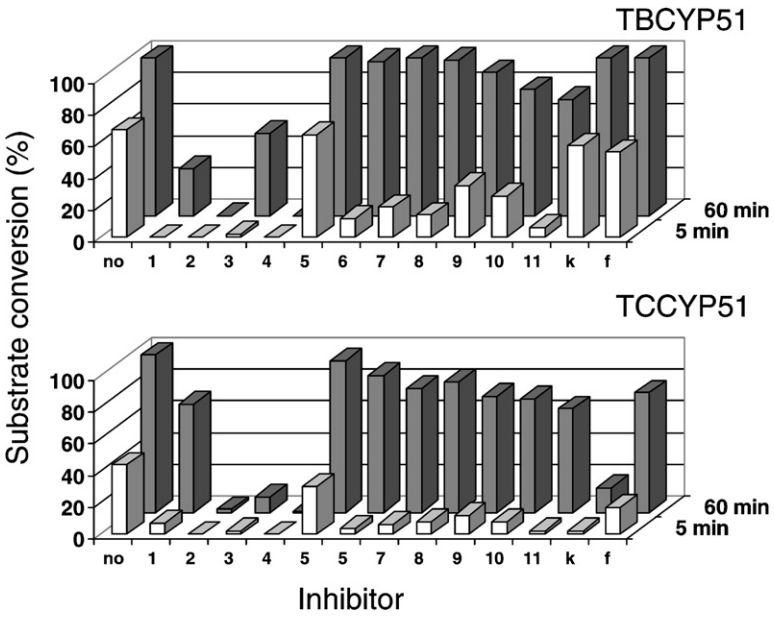

Figure 3. CYP51 Activity at 1:1 Molar Ratio Inhibitor/Enzyme

The substrates are added at 50-fold molar excess. The results are presented as mean; standard deviation (SD) did not exceed 10%. Inhibitor numbers and letters refer to compounds in Figure 2.

indicated that the heme-coordinated imidazole nitrogen of compound **10** is much more easily replaced by CO from the iron coordination sphere.

One explanation of the data is that the affinity of azole-CYP51 interaction in the reaction mixture can be altered, the expression of the differences depending on the inhibitor structure. The number of contacts between the azole molecule and the enzyme substrate binding cavity might be decreased as a result of protein conformational dynamics upon substrate recognition, interaction with the reductase, electron transfer, and subsequent reduction so that inhibitors such as **10** can be more easily released from the active center. An alternative explanation can be connected with the fact that binding of some inhibitors alone is known to cause conformational changes in P450s [44]. By tightening the complex, such changes might impede protein dynamics and thus make the inhibitory effect much stronger, for example as with **4**. To summarize, being a useful tool in the primary search for binding ligands, spectral response of substrate-free oxidized P450 may not truly reflect the relative affinity of the interaction under the reaction conditions. Prediction of the inhibitory potency relying solely on binding parameters or IC_{50} values determined as the influence on the initial rate of reaction (especially without considering P450 concentration) can be misleading. Long-term inhibitory effect appears to be most informative for identification of strongest CYP51 inhibitors.

Azole Structure/Activity Relationship

The two strongest TB and TC CYP51 inhibitors (**2** and **4**) (Figure 2A) differ in composition of the substituents at the δ-position relative to the imidazole, yet both contain a phenyl ring at the β-position. The inhibitory effect of the levorotatory enantiomer of **2** (compound **3**) is slightly weaker, but the I/E_2 ratios after extended incubation with CYP51 still remain less than 1. On the contrary, in all inhibitors that revealed sharp time-dependent increase in the I/E_2 values (**5–10**) the phenyl group is present at the α-position. Because structurally the α-phenyl compounds differ only in the composition on the δ-substituents, influence of these differences on the apparent binding affinity can be easily seen. While a short five-member heterocycle of **5** is clearly insufficient to provide efficient binding, bulkier constituents (**6–10**) produce better K_d values. When this part of the molecule consists of two aromatic rings with rigid connection (**6**, **7**), the calculated affinities remain moderate,

Table 1. Modification of Azole-Binding Properties upon Substrate Binding or Heme Reduction and Replacement of the Bound Azoles by Substrate or Carbon Monoxide

Selected Azoles	Apparent K_d, μM: Oxidized, No Substrate	Apparent K_d, μM: Oxidized, Plus Substrate[a]	Apparent K_d, μM: Reduced, No Substrate	Replacement by Substrate (% of high-spin form)	Replacement by CO (versus no inhibitor), %[b]: Rate (per minute)	Replacement by CO (versus no inhibitor), %[b]: Maximum
4	0.05 ± 0.003	0.17 ± 0.02 (3↑)	0.07 ± 0.01 (1.6↑)	-	6 ± 0.7	52 ± 7
10	0.05 ± 0.002	2.2 ± 0.44 (44↑)	0.26 ± 0.02 (4↑)	+ (34 ± 0.7)	13 ± 0.8	95 ± 6

[a] Obtusifoliol, 20μM (azole titration range 0.2–10 μM).
[b] The spectra are shown in Figure S2. The results of two experiments are presented as mean ± standard error.

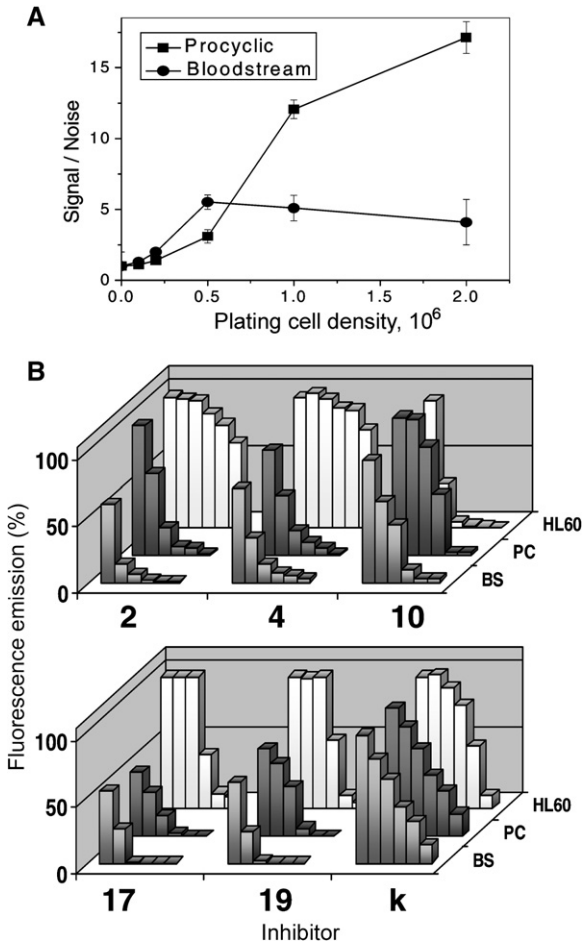

Figure 4. Growth and Inhibition of TB

(A) Sensitivity of Alamar Blue assay to monitor viable TB cells: the ratios between fluorescence emission in growing cells (signal) and in the growth media (noise) at increasing plating densities of procyclic and bloodstream TB. Error bars represent SD.

(B) Cellular responses to the CYP51 inhibitors (1, 5, 10, 20, 30, and 50 μM) BS, bloodstream TB, PC, procyclic TB, HL60, human leukemia cell line. Effects of the compounds on the Alamar Blue absorbance spectra are shown in Figure S4.

but when the connection is flexible (especially **9** and **10**) the K_ds become very low, the best values (0.05 μM) being as good as those obtained for compound **4**. Perhaps flexibility of this part of the azole molecule leads to its easier entry into the CYP51 substrate binding cavities, but similar to the other α-phenyl azoles, it still lacks restraining interactions necessary to prevent the inhibitors from being replaced by the substrate upon catalysis. On the other hand, compounds **1** and **11,** having α-substituents more bulky than a single phenyl ring, produce long-term inhibitory effects stronger than **5–10** (Figure 2A). In addition, these two azoles demonstrate some selectivity. Compound **1** (two phenyl rings at the α-position) is a little more favorable for TBCYP51, while for TCCYP51, the longer arm of the benzyl group (so that benzene and imidazole rings remain separated by two C atoms) of **11** is preferable.

Modification of a Basic Structure

Because any drug development process can face problems such as cytotoxicity, cell permeability, solubility, rapid turnover in plasma, insufficient life-time, etc., it is important to be able to predict the most promising directions for further modifications of a lead structure. To verify the importance of the phenyl group location at the β versus the α position, the α-phenyl isomer of **4** (compound **12**) (Figure 2B) was tested and, in correspondence with our predictions from compounds **6–10**, regardless of its strong apparent binding affinity, showed a rapid decrease in the inhibitory effect over time. Influence of alteration in the composition of the β-substituent was investigated with an additional set of eight derivatives of compound **4.** The inhibitory effects were compared as inhibition of CYP51 activity at 1:1 molar ratio azole/P450 after 5 and 60 min reaction, and quite significant differences in their potencies were observed (Figure S3). Two of these compounds (**17** and **19**) (Figure 2B), revealed inhibitory effects as strong as **4** and were included in further studies.

Correlation between CYP51 Inhibition and Antiparasitic Effect

Cellular Responses in the Mammalian and Insect Life Stages of TB

Only two of four clinically available drugs (melarsoprol and eflornithine [Figure S1]) can treat late stages of sleeping sickness. However, eflornithine is only efficient for TB *gambiense*, and melarsoprol is extremely toxic, causing severe, often fatal encephalopathy, and has up to 30% resistance in parts of central Africa. Suramin and pentamidine do not penetrate the blood/brain barrier and can treat only the first, hemolymphatic stage of the disease, which sometimes passes unnoticed because of nonspecific symptoms. Recently quite promising data on use of nitroimidazoles as possible drug candidates for African trypanosomiasis have been reported [46], yet the target for these compounds has not been determined. Though major sterol components identified in bloodstream TB most likely originate from host cholesterol [27], it is not excluded that the parasite might still require functional sterols, for which hormonal level of action can be below routine sterol detection limits. We aimed to clarify this issue by comparison of the effects of potent TBCYP51 inhibitors in bloodstream and procyclic (known to synthesize endogenous sterols [27, 47]) cells of TB.

The Alamar Blue method was adjusted to monitor TB cell growth. While the procyclic form, though growing slowly at low concentrations provided very good fluorescent signal starting from plating density of 10^6 cells/ml (Figure 4A) for the bloodstream TB originally cultured in the commonly used HMI-9 medium [48], the signal/noise ratios remained below 2 and rapidly dropped over time with increase in the cell densities. Using absorbance spectroscopy, we have observed that several components of the HMI-9 themselves cause fast Alamar Blue reduction and that the bloodstream TB can further convert the reduced (fluorescent) dye into its colorless hydroxy

Table 2. Sensitivities of Trypanosomal Cells to CYP51 Inhibitors

	TB Testing System				TC Testing System			
	ED_{50}, μM[a]				Trypomastigotes		Amastigotes	
CYP51 Inhibitor	Procyclic TB	Bloodstream TB	HumanHL60	Selectivity Index[b]	ED_{50}, μM	Inhibition at 1 μM, %	ED_{95}, μM	Inhibition at 1 μM, %
K[c]	18	16	29	1.8	nt[d]	-	-	-
2	7	1.3	>50	>38	<1	78	<1	99
4	4	2.5	>50	>20	<1	72	<1	97
10	20	8	4	0.5	8	7	20	43
17	1	1.3	20	15	nt	-	-	-
19	5	1.5	22	15	<1	92	<1	99

The values were calculated from the dose-response curves.
[a] The dose causing a 50% cell growth inhibition, $ED_{50} < 10$ μM being proposed as a threshold to consider a compound as a potential antisleeping sickness drug [45].
[b] $ED_{50(HL60)}/ED_{50(bloodstream\ TB)}$.
[c] Ketoconazole.
[d] Not tested.

form [49]. To overcome this problem, several different cell culture media were tested, and RPMI 1640 found to combine both requirements, support bloodstream TB growth and maintain the dye in the oxidized nonfluorescent form, was used in further experiments.

All the azoles demonstrated clear dose-dependent inhibitory effect on both procyclic and bloodstream TB (Figure 4B). Among them, ED_{50} above 10 μM for bloodstream TB was obtained only for ketoconazole (35% and 37% responses for procyclic and bloodstream TB, respectively, with less than 10% negative influence on human HL60). At increasing ketoconazole concentration, inhibition of human cells becomes more pronounced, selectivity index human/bloodstream TB being 1.8 (Table 2). This low selectivity is not surprising for ketoconazole since the drug is known to inhibit growth of cancer cells and has been used for a long time in cancer chemotherapy [50, 51]. Though stronger effect of **10** in bloodstream versus procyclic TB (8 and 20 μM, respectively) may reflect slower sterol flow (which means lower concentration of the CYP51 substrate) in the mammalian form of the parasite, most likely a large portion of sensitivity of the TB cells to **10** might result from general cytotoxicity of the compound unless the effect on HL60 is cancer cell specific. The best antitrypanosomal activity is provided by the four strongest CYP51 inhibitors, compounds **2**, **4**, **17**, and **19**. At 10 μM concentration, these azoles cause more than 90% growth inhibition of bloodstream TB, three of them produce ED_{50} below 2 μM. The observed direct correlation between the potency of the tested azoles as CYP51 inhibitors and their antiparasitic effect both in insect and mammalian stages of the TB lifecycle indicates that CYP51 reaction is essential in the bloodstream form of the parasite and thus supports the notion [10] that sparking sterols may play an important role in *Trypanosomatidae*. High selectivity of compounds **2**, **4**, **17**, and **19** for trypanosomal cells makes them good candidates for further testing as potential antitrypanosomal agents.

Effect on TC: Bloodstream Trypomastigotes and Intracellular Amastigotes

Both clinical drugs currently available for treatment of TC infections (benzinidazole and nifutrimox [Figure S1]) are effective only for the early stages, intracellular forms of TC being more difficult targets. Because human stages of TC are known to synthesize endogenous sterols with the major component being the final sterol product of the fungal pathway, ergosterol, azole derivatives were tested as potential anti-TC agents. Some of them were found effective and are considered for clinical trials [18–20]. However, specific inhibition of the target enzyme has never been investigated.

Potent TCCYP51 inhibitors produce profound antiparasitic effect on TC (Figure 5 and Table 2). The ability of trypomastigotes to infect heart cells after exposure to 1 μM concentration of **2**, **4**, and **19** was decreased by 78%, 72%, and 92%, respectively (Figure 5A, lower panel). Only for compound **10** (short-term TCCYP51 inhibitor) 8 μM concentration was required to reach 50% inhibition. Most remarkably, the compounds strongly inhibit multiplication of amastigotes within cardiomyoblasts, ED_{95} being less than 1 μM for **2**, **4**, and **19** (inhibition at 1 μM 99%, 97%, and 99%, respectively) as seen in Figure 5A, upper panel, and microscopically observed in Figure 5B, suggesting their potential applicability to be used for treatment of currently incurable late stages of the disease. Alterations in the sterol composition of TC cells upon treatment with compound **2** (sharp decrease in the ergosterol formation and accumulation of the C14 methylated precursors 24-methylenedihydrolanosterol and lanosterol) (Figure 5C) provide direct evidence that the mode of action of the compound is connected with CYP51 inhibition.

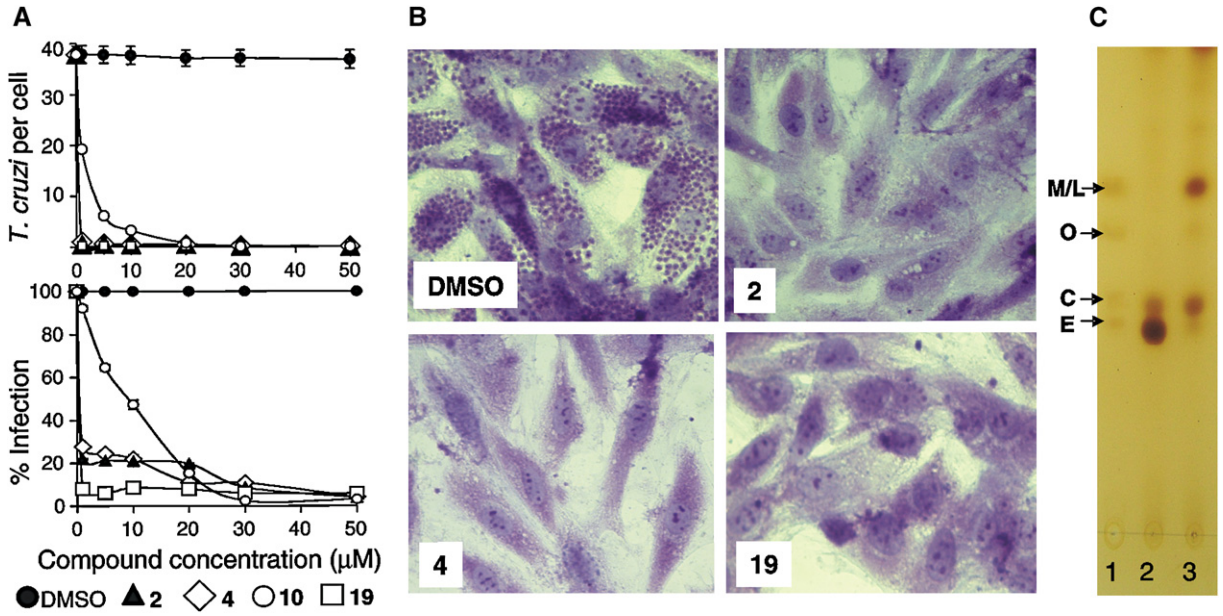

Figure 5. Exposure of *T. cruzi* Trypomastigotes to CYP51 Inhibitors Dramatically Inhibits *T. cruzi* Multiplication within Cardiomyocytes and the Percentage of Cellular Infection

(A) Potent inhibition of both *T. cruzi* intracellular multiplication and infection in cardiomyoblasts by CYP51 inhibitors. Trypomatigotes were pretreated with several concentrations of CYP51 inhibitors **2**, **4**, **10**, and **19** or mock treated, exposed to cardiomyoblasts monolayers, and *T. cruzi* multiplication was evaluated at 72 hr by determining the number of *T. cruzi*/cell (upper insert) and the percent of infection (lower insert). The data represent the mean ± SD of results from triplicate samples. SD did not exceed 10% of the mean.

(B) Microscopic observation of the inhibition of *T. cruzi* multiplication by 1 μM CYP51 inhibitors within cardiomyoblasts at 72 hr. *T. cruzi* pretreated with control DMSO showed high levels of parasite multiplication, whereas cells exposed to trypanosomes preincubated with 1 μM azoles showed dramatic decrease in the number of intracellular parasites.

(C) TLC analysis of sterol composition of TC cells. Sterol standards: 24-methylenedihydrolanosterol (M), lanosterol (L), obtusifoliol (O), cholesterol (C), and ergosterol (E), 5 nmoles each (lane 1). Sterols from 10 mg of cell pellet of untreated epimastigotes (lane 2) and epimastigotes incubated for 120 hr with compound **2** (lane 3). The results of GC-MS analysis of TC sterols are provided in Table S2.

SIGNIFICANCE

Because TB species contain only two *CYP* genes, encoding CYP51 and a putative P450 of unknown function (http://www.tigr.org/), antiparasitic effect of potent CYP51 inhibitors in TB must be directly connected with disturbances in sterol 14α-demethylation. Comparable sensitivities of bloodstream and procyclic TB to the TBCYP51 inhibitors imply that the *CYP*51 gene is active in the mammalian stages of the parasite lifecycle and thus support the notion [29] that, similar to plants/algae, biologically active (functional) sterols of endogenous nature must be essential in *Trypanosomatidae.* This finding suggests that CYP51 inhibitors should be included in testing as potential antisleeping sickness agents and that the nitroimidazoles, recently found to be potent in killing bloodstream TB [46], might actually target TBCYP51. Supported by the profound effect of the most potent TCCYP51 inhibitors both in trypomastigote and intracellular human stages of TC, the work offers a novel lead structure with a defined region most promising for possible further modifications for antitrypanosomal therapy. Taking into account high amino acid sequence identity between the CYP51s from *Trypanosoma and Leishmania* (74%–78%) there is a high probability that the same compounds will be effective against leishmaniasis, which might be of vital importance for visceral forms of the disease as many azoles are known to penetrate the blood/brain barrier [52]. The approach undertaken in this study including large-scale spectroscopic screening for binding ligands and quantification of the inhibitory potencies in the reconstituted enzyme reaction followed by testing the best compounds in the parasite cells is promising to follow for the discovery of new, rationally designed antiprotozoan drugs and perhaps novel antifungal agents as well.

EXPERIMENTAL PROCEDURES

Overexpression of TB and TC CYP51 in *E. coli*, purification to electrophoretic homogeneity, and reconstitution of enzymatic activities with ^{3}H-labeled sterol substrates were performed as previously described [31, 32]. Experimental azole derivatives and their further modifications were a generous gift from Novartis Research Institute (Vienna, Austria); the Novartis numbers for the compounds are: **1**, SDZ-89443(−), **2**, SDZ-284692(+); **3**, SDZ-284693(−); **4**, SDZ-285604(−); **5**, SDZ-287113; **6**, VAB251(R); **7**, VAB309(R); **8**, SDZ-287115; **9**, VAB636(R); **10**, VAB635(R); **11**, SDZ-285936; **12**, SDZ-285428(S); **17**, SDZ-284531; **19**, SDZ-284797(+); **20**, SDZ-284798(−).

Spectroscopic Titration of TB and TCCYP51 with Azoles

Azole-induced spectral changes in TC and TBCYP51 (2 μM) were monitored in 2 ml tandem cuvettes in the wavelength range 350–500 nm with a Shimadzu UV-2401PC spectrophotometer. The azoles were dissolved in DMSO (1 mM) and added in the range 0.2–20 μM. Maximal spectral response per nanomole of P450 ($\Delta A_{426-410}$ for oxidized substrate free, $\Delta A_{426-390}$ for oxidized CYP51 in presence of substrate, and $\Delta A_{424-445}$ for reduced, substrate-free CYP51) and apparent K_d were determined from the equilibrium titration curves (Figure 1, insert) by plotting absorbance changes against the concentration of free ligand and fitting the data to a rectangular hyperbola with SigmaPlot Statistics [53]. Replacement of the azoles by sterol substrate and by carbon monoxide after the titration experiments was monitored as type 1 spectral response and as CO binding spectra, respectively.

Inhibition of CYP51 Activity

Equal volumes of the reaction mixture containing 1 μM P450, 2 μM TB cytochrome P450 reductase, 50 μM obtusifoliol for TBCYP51, and 24-methylenedihydrolanosterol for TCCYP51 were added to the tubes with the azole inhibitors (final concentration 1–100 μM), and the reaction was initiated with the addition of NADPH. For time-course measurements, aliquots of the reaction mixture were taken over time. The sterols were extracted with ethyl acetate and analyzed by reverse phase HPLC equipped with β-RAM radioactivity flow detector by using Nova-Pak C18 column. Reverse phase HPLC with 0.05 M disodium hydrogen orthophosphate/acetonitrile (50:50 v/v) adjusted to pH 6.0 with glacial acetic acid as the mobile phase and UV detection at 230 nm was employed to confirm stability of the azoles in the solution during the reaction. CO-spectra of the control (no inhibitor) sample were taken to confirm stability of the P450s. The inhibitory potencies of azoles were compared upon time course measurements as I/E_2 (molar ratio inhibitor/enzyme at which the substrate conversion decreases 2-fold) and as percentage of inhibition at molar ratio 1:1.

Cell Culture and Growth Inhibition Assay for TB

The procyclic forms of the TB cell line 29-13 were grown in SDM-79 medium (JRH Biosciences, Lenox, KS) supplemented with 10% heat-inactivated fetal bovine serum at 27°C [54]. Bloodstream forms of the TB cell line SM427 [48] and human myeloid leukemia cells HL60 (DSZM, Braunschweig, Germany) were grown in RPMI 1640 medium supplemented with 10% heat-inactivated fetal bovine serum at 37°C. Both cultures were maintained in a humidified atmosphere containing 5% CO_2. Cell counting was done with a Neubauer haemocytometer. The cells were seeded at various densities (10^5–2×10^6/ml) in 24-well plates and incubated for 48 hours. The cell viability indicator Alamar Blue (Biosource, USA) was added to final concentration of 10%, and after 2 hr of additional incubation, 200 μl aliquots were placed into 96-well flat bottom microtiter plates (Costar, USA), and fluorescence was measured at 520 nm excitation wavelength and 590 nm emission wavelength by using a FLUOstar Optima plate reader (BMG Lab Technologies, Germany). Cell viability was monitored as emission in the cells versus emission in the growth media (signal-to-noise ratio). Plating cell densities of 10^6 for the procyclic forms and 5×10^5 for the bloodstream forms of TB and for human HL60 (signal-to-noise ratios 12, 6, and 4.5, respectively) were selected for further measurements. Reduction of Alamar Blue in the cells, absence of media-induced reduction or further conversion into the hydro form were confirmed by absorbance spectroscopy in the range of 400–700 nm (the spectra are shown as Figure S4). To evaluate the growth inhibition effect, the cells were incubated in the presence of CYP51 inhibitors (0–50 μM), the antisleeping sickness drug suramin (bloodstream TB), and NaN_3 (procyclic TB). Wells containing cells, medium, and 1% DMSO alone served as controls. The concentrations causing 50% growth inhibition (ED_{50}, 50% effective dose) were calculated from dose-response curves. The selectivity of the inhibitors for the parasite cells was estimated as ratio ED_{50} (human HL60)/ED_{50} (bloodstream TB) [45].

Growth and Inhibition of TC

Trypomastigotes (10^6 organisms) were pre-exposed to the CYP51 inhibitors 2, 4, 10, and 19 dissolved in DMSO/DMEM at several concentrations (1–50 μM) or to control DMSO/DMEM for 30 min. The parasites were then exposed in triplicate to rat cardiomyocyte monolayers at the ratio 10 parasites/cell in Lab Tech chambers for 2 hr as described [55]. After removing the unbound parasites, monolayers were incubated with DMEM supplemented with 10% FBS for 72 hr to allow parasite intracellular multiplication and the number of *T. cruzi* per 200 cells, and the percent of infection were microscopically determined in Giemsa stained monolayers [55].

TLC and GC-MS Analysis of TC Sterols

Epimastigotes (plating density 10^7 cells/ml) were cultured in brain heart infusion supplemented with hemin and 10% calf serum for 120 hr without an inhibitor and in the presence of compound **2**. The inhibitor was added daily to maintain 1 μM concentration for the first 3 days, and 2 μM concentration for the last 2 days. The cell pellet was washed with Hank's balanced salt solution without phenol red to remove excess of cholesterol from the serum and saponified by using 10% KOH in 98% aqueous methanol at reflux temperature for 1 hr. The neutral lipids obtained by dilution with water and extraction with hexane were subjected to silica gel TLC plates (0.25 μm, Whatman, Germany) for 30 min in hexane:ethyl acetate (8:2) as developing solvent and monitored in an iodine chamber. Individual sterols were identified by using a GC-MS apparatus with Hewlett-Packard LS 6500 gas chromatograph interfaced to a 5973 mass spectrometer as described previously [29].

Supplemental Data

Supplemental Data include binding of the azoles to the CYP51 orthologs from human and *Mycobacterium tuberculosis*, list of clinical drugs currently used for antitrypanosomal therapy, CO-binding spectra of TBCYP51 in the presence and in the absence of inhibitors **4** and **10**, inhibitory effects on the CYP51 activity of the compounds obtained upon structure **4** modification, absorbance spectra of Alamar Blue upon reduction by TB cells, and GC-MS data on sterol composition of TC cells grown in the absence and in the presence of compound **2** and are available at http://www.chembiol.com/cgi/content/full/14/11/1283/DC1/.

ACKNOWLEDGMENTS

This work was supported by grants from the National Institutes of Health (GM067871 to M.R.W., GM63477 to W.D.N., SC1GM 081168 and GM 008037 to F.V.), from the American Heart Association (0535121N to G.I.L.), and from Welch Foundation (D-1276 to W.D.N.).

Received: June 15, 2007
Revised: October 12, 2007
Accepted: October 15, 2007
Published: November 26, 2007

REFERENCES

1. Barrett, M.P., Burchmore, R.J., Stich, A., Lazzari, J.O., Frasch, A.C., Cazzulo, J.J., and Krishna, S. (2003). The trypanosomiases. Lancet *362*, 1469–1480.
2. (2006). Chagas' disease—an epidemic that can no longer be ignored. Lancet *368*, 619.
3. Newsome, A.L., and McGhee, C.R. (2006). *Trypanosoma cruzi* in Triatomes from an urban and domestic setting in Middle Tennessee. J. Ten. Acad. Sci. *81*, 62–65.
4. Diaz, J.H. (2007). Chagas disease in the United States: a cause for concern in Louisiana? J. La. State Med. Soc. *159*, 21–23, 25–29.
5. Morel, C.M., and Lazdins, J. (2003). Chagas disease. Nat. Rev. Microbiol. *1*, 14–15.

6. Luscher, A., de Koning, H.P., and Maser, P. (2007). Chemotherapeutic strategies against *Trypanosoma brucei*: drug targets vs. drug targeting. Curr. Pharm. Des. *13*, 555–567.

7. El-Sayed, N.M., Myler, P.J., Blandin, G., Berriman, M., Crabtree, J., Aggarwal, G., Caler, E., Renauld, H., Worthey, E.A., Hertz-Fowler, C., et al. (2005). Comparative genomics of trypanosomatid parasitic protozoa. Science *309*, 404–409.

8. Croft, S.L., Barrett, M.P., and Urbina, J.A. (2005). Chemotherapy of trypanosomiases and leishmaniasis. Trends Parasitol. *21*, 508–512.

9. Nes, W.R., and McKean, M.R. (1977). Biochemistry of Steroids and Other Isopentenoids (Baltimore: University Park Press).

10. Roberts, C.W., McLeodm, R., Rice, D.W., Ginger, M., Chance, M.L., and Goad, L.J. (2003). Fatty acid and sterol metabolism: potential antimicrobial targets in apicomplexan and trypanosomatid parasitic protozoa. Mol. Biochem. Parasitol. *126*, 129–142.

11. Vanden Bossche, H., Koymans, L., and Moereels, H. (1995). P450 inhibitors of use in medical treatment: focus on mechanisms of action. Pharmacol. Ther. *67*, 79–100.

12. Gupta, A.K., and Tomas, E. (2003). New antifungal agents. Dermatol. Clin. *21*, 565–576.

13. Docampo, R., Moreno, S.N., Turrens, J.F., Katzin, A.M., Gonzalez-Cappa, S.M., and Stoppani, A.O. (1981). Biochemical and ultrastructural alterations produced by miconazole and econazole in *Trypanosoma cruzi*. Mol. Biochem. Parasitol. *3*, 169–180.

14. Lazardi, K., Urbina, J.A., and de Souza, W. (1990). Ultrastructural alterations induced by two ergosterol biosynthesis inhibitors, ketoconazole and terbinafine, on epimastigotes and amastigotes of *Trypanosoma (Schizotrypanum) cruzi*. Antimicrob. Agents Chemother. *34*, 2097–2105.

15. Urbina, J.A., Payares, G., Molina, J., Sanoja, C., Liendo, A., Lazardi, K., Piras, M., Piras, R., Perez, N., Wincker, P., and Ryley, J.F. (1996). Cure of short- and long-term experimental Chagas' disease using D0870. Science *273*, 969–971.

16. Apt, W., Aguilera, X., Arribada, A., Perez, C., Miranda, C., Sanchez, G., Zulantay, I., Cortes, P., Rodriguez, J., and Juri, D. (1998). Treatment of chronic Chagas' disease with itraconazole and allopurinol. Am. J. Trop. Med. Hyg. *59*, 133–138.

17. Araujo, M.S., Martins-Filho, O.A., Pereira, M.E., and Brener, Z. (2000). A combination of benznidazole and ketoconazole enhances efficacy of chemotherapy of experimental Chagas' disease. J. Antimicrob. Chemother. *45*, 819–824.

18. Molina, J., Martins-Filho, O., Brener, Z., Romanha, A.J., Loebenberg, D., and Urbina, J.A. (2000). Activities of the triazole derivative SCH 56592 (posaconazole) against drug-resistant strains of the protozoan parasite *Trypanosoma (Schizotrypanum) cruzi* in immunocompetent and immunosuppressed murine hosts. Antimicrob. Agents Chemother. *44*, 150–155.

19. Urbina, J.A. (2001). Specific treatment of Chagas disease: current status and new developments. Curr. Opin. Infect. Dis. *14*, 733–741.

20. Buckner, F., Yokoyama, K., Lockman, J., Aikenhead, K., Ohkanda, J., Sadilek, M., Sebti, S., Van Voorhis, W., Hamilton, A., and Gelb, M.H. (2003). A class of sterol 14-demethylase inhibitors as anti-*Trypanosoma cruzi* agents. Proc. Natl. Acad. Sci. USA *100*, 15149–15153.

21. Urbina, J.A., Concepcion, J.L., Caldera, A., Payares, G., Sanoja, C., Otomo, T., and Hiyoshi, H. (2004). In vitro and in vivo activities of E5700 and ER-119884, two novel orally active squalene synthase inhibitors, against Trypanosoma cruzi. Antimicrob. Agents Chemother. *48*, 2379–2387.

22. Hucke, O., Gelb, M.H., Verlinde, C.L., and Buckner, F.S. (2005). The protein farnesyltransferase inhibitor Tipifarnib as a new lead for the development of drugs against Chagas disease. J. Med. Chem. *48*, 5415–5418.

23. Gebre-Hiwot, A., and Frommel, D. (1993). The in-vitro anti-leishmanial activity of inhibitors of ergosterol biosynthesis. J. Antimicrob. Chemother. *32*, 837–842.

24. Haughan, P.A., Chance, M.L., and Goad, L.J. (1995). Effects of an azasterol inhibitor of sterol 24-transmethylation on sterol biosynthesis and growth of *Leishmania donovani* promastigotes. Biochem. J. *308*, 31–38.

25. Rodrigues, J.C.F., Urbina, J.A., and de Souza, W. (2005). Antiproliferative and ultrastructural effects of BPQ-OH, a specific inhibitor of squalene synthase, on *Leishmania amazonensis*. Exp. Parasitol. *111*, 230–238.

26. Coppens, I., Baudhuin, P., Opperdoes, F.R., and Courtoy, P.J. (1988). Receptors for the host low density lipoproteins on the hemoflagellate *Trypanosoma brucei*: purification and involvement in the growth of the parasite. Proc. Natl. Acad. Sci. USA *85*, 6753–6757.

27. Coppens, I., and Courtoy, P.J. (2000). The adaptative mechanisms of *Trypanosoma brucei* for sterol homeostasis in its different life-cycle environments. Annu. Rev. Microbiol. *54*, 129–156.

28. Lorente, S.O., Rodrigues, J.C., Jimenez, C., Joyce-Menekse, M., Rodrigues, C., Croft, S.L., Yardley, V., de Luca-Fradley, K., Ruiz-Perez, L.M., and Urbina, J. (2004). Novel azasterols as potential agents for treatment of leishmaniasis and trypanosomiasis. Antimicrob. Agents Chemother. *48*, 2937–2950.

29. Zhou, W., Cross, G.A., and Nes, W.D. (2007). Cholesterol import fails to prevent catalyst-based inhibition of ergosterol synthesis and cell proliferation of Trypanosoma brucei. J. Lipid Res. *48*, 665–673.

30. Lepesheva, G.I., and Waterman, M.R. (2007). Sterol 14alpha-demethylase cytochrome P450 (CYP51), a P450 in all biological kingdoms. Biochim. Biophys. Acta *1770*, 467–477.

31. Lepesheva, G.I., Nes, W.D., Zhou, W., Hill, G.C., and Waterman, M.R. (2004). CYP51 from *Trypanosoma brucei* is obtusifoliol-specific. Biochemistry *43*, 10789–10799.

32. Lepesheva, G.I., Zaitseva, N.G., Nes, W.D., Zhou, W., Arase, M., Liu, J., Hill, G.C., and Waterman, M.R. (2006). CYP51 from *Trypanosoma cruzi*: a phyla-specific residue in the B′ helix defines substrate preferences of sterol 14alpha-demethylase. J. Biol. Chem. *281*, 3577–3585.

33. Lepesheva, G.I., Hargrove, T.Y., Ott, R.D., Nes, W.D., and Waterman, M.R. (2006). Biodiversity of CYP51 in trypanosomes. Biochem. Soc. Trans. *34*, 1161–1164.

34. Ortiz de Montellano, P.R., and Correia, M.A. (1995). Inhibition of cytochrome P450 enzymes. In Cytochrome P450: Structure, Mechanism, and Biochemistry, P.R. Ortiz de Montellano, ed. (New York: Plenum Publishing Corp.), pp. 305–364.

35. Zhang, W., Ramamoorthy, Y., Kilicarslan, T., Nolte, H., Tyndale, R.F., and Sellers, E.M. (2002). Inhibition of cytochromes P450 by antifungal imidazole derivatives. Drug Metab. Dispos. *30*, 314–318.

36. Marichal, P., Koymans, L., Willemsens, S., Bellens, D., Verhasselt, P., Luyten, W., Borgers, M., Ramaekers, F.C., Odds, F.C., and Bossche, H.V. (1999). Contribution of mutations in the cytochrome P450 14alpha-demethylase (Erg11p, Cyp51p) to azole resistance in *Candida albicans*. Microbiology *145*, 2701–2713.

37. Schiaffella, F., Macchiarulo, A., Milanese, L., Vecchiarelli, A., and Fringuelli, R. (2006). Novel ketoconazole analogues based on the replacement of 2,4-dichlorophenyl group with 1,4-benzothiazine moiety: design, synthesis, and microbiological evaluation. Bioorg. Med. Chem. *14*, 5196–5203.

38. Sun, Q.Y., Xu, J.M., Cao, Y.B., Zhang, W.N., Wu, Q.Y., Zhang, D.Z., Zhang, J., Zhao, H.Q., and Jiang, Y.Y. (2007). Synthesis of

novel triazole derivatives as inhibitors of cytochrome P450 14alpha-demethylase (CYP51). Eur. J. Med. Chem. *42*, 1226–1233.

39. Munayyer, H.K., Mann, P.A., Chau, A.S., Yarosh-Tomaine, T., Greene, J.R., Hare, R.S., Heimark, L., Palermo, R.E., Loebenberg, D., and McNicholas, P.M. (2004). Posaconazole is a potent inhibitor of sterol 14alpha-demethylation in yeasts and molds. Antimicrob. Agents Chemother. *48*, 3690–3696.
40. Rogers, T.R. (2006). Antifungal drug resistance: limited data, dramatic impact? Int. J. Antimicrob. Agents *27*, 7–11.
41. Schuster, I., Egger, H., Nussbaumer, P., and Kroemer, R.T. (2003). Inhibitors of vitamin D hydroxylases: structure-activity relationships. J. Cell. Biochem. *88*, 372–380.
42. Schuster, I., Egger, H., Astecker, N., Herzig, G., Schussler, M., and Vorisek, G. (2001). Selective inhibitors of CYP24: mechanistic tools to explore vitamin D metabolism in human keratinocytes. Steroids *66*, 451–462.
43. Omura, T., and Sato, R. (1964). The carbon monoxide-binding pigment of liver microsomes. II. Solubilization, purification, and properties. J. Biol. Chem. *239*, 2379–2385.
44. Yano, J.K., Denton, T.T., Cerny, M.A., Zhang, X., Johnson, E.F., and Cashman, J.R. (2006). Synthetic inhibitors of cytochrome P-450 2A6: inhibitory activity, difference spectra, mechanism of inhibition, and protein cocrystallization. J. Med. Chem. *49*, 6987–7001.
45. Hoet, S., Opperdoes, F., Brun, R., and Quetin-Leclercq, J. (2004). Natural products active against African trypanosomes: a step towards new drugs. Nat. Prod. Rep. *21*, 353–364.
46. Torreelee, E. (2007). Rediscovering nitro-imidazoles as promising drug candidates for human African Trypanosomiasis. Drugs Against Protozoan Parazites, Keystone Symposia on Molecular and Cellular Biology, Tahoe City, CA, pp. 36.
47. Dixon, H., Ginger, C.D., and Williamson, J. (1972). Trypanosome sterols and their metabolic origins. Comp. Biochem. Physiol. B *41*, 1–18.
48. Carruthers, V.B., and Cross, G.A. (1992). High-efficiency clonal growth of bloodstream- and insect-form *Trypanosoma brucei* on agarose plates. Proc. Natl. Acad. Sci. USA *89*, 8818–8821.
49. O'Brien, J., Wilson, I., Orton, T., and Pognan, F. (2000). Investigation of the Alamar Blue (resazurin) fluorescent dye for the assessment of mammalian cell cytotoxicity. Eur. J. Biochem. *267*, 5421–5426.
50. Wang, Y.J., Jeng, J.H., Chen, R.J., Tseng, H., Chen, L.C., Liang, Y.C., Lin, C.H., Chen, C.H., Chu, J.S., Ho, W.L., and Ho, Y.S. (2002). Ketoconazole potentiates the antitumor effects of nocodazole: In vivo therapy for human tumor xenografts in nude mice. Mol. Carcinog. *34*, 199–210.
51. Dyrstad, S.W., Shah, P., and Rao, K. (2006). Chemotherapy for prostate cancer. Curr. Pharm. Des. *12*, 819–837.
52. Goodpasture, H.C., Hershberger, R.E., Barnett, A.M., and Peterie, J.D. (1985). Treatment of central nervous system fungal infection with ketoconazole. Arch. Intern. Med. *145*, 879–880.
53. Lepesheva, G.I., Virus, C., and Waterman, M.R. (2003). Conservation in the CYP51 family. Role of the B′ helix/BC loop and helices F and G in enzymatic function. Biochemistry *42*, 9091–9101.
54. Hirumi, H., Hirumi, K., Moloo, S.K., and Shaw, M.K. (1992). *Trypanosoma brucei brucei*: in vitro production of metacyclic forms. J. Protozool. *39*, 619–627.
55. Nde, P.N., Simmons, K.J., Kleshchenko, Y., Pratap, S., Lima, M.F., and Villalta, F. (2006). Silencing of the laminin γ-1 gene blocks *Trypanosoma cruzi* infection. Infect. Immun. *74*, 1643–1648.